Present Day Stress Orientation in Brunei: A Snapshot of 'Prograding Deltaic Tectonics'

MARK R. P. TINGAY[1], RICHARD R. HILLIS[2], CHRIS K. MORLEY[3] RICHARD E. SWARBRICK[4], STEVE J. DRAKE[5]

[1] *Australian School of Petroleum, University of Adelaide, Adelaide, Australia. Now at: World Stress Map Project, Geophysics Institute, University Karlsruhe, Karlsruhe, Germany.*

mark.tingay@gpi.uni-karlsruhe.de

[2]*Australian School of Petroleum, University of Adelaide, Adelaide, Australia.*

[3]*University of Brunei Darussalam, Bandar Seri Begawan, Negara Brunei Darussalam.*

[4]*Durham University, Durham, United Kingdom.*

[5]*Brunei Shell Petroleum, Seria, Negara Brunei Darussalam.*

6302 Words (including references and figure captions), 14 figures.

Running header: 'Prograding deltaic tectonics' in Brunei

ABSTRACT

The Baram Delta province of northwest Borneo is unusual when compared to other Tertiary deltas, as it has built up upon an active margin. Hence, structures observed in the Baram Delta province are the result of both margin-parallel gravity-driven deltaic tectonics and approximately margin-normal transpressive tectonics associated with the active margin. Image and dipmeter logs have been examined for breakouts and drilling-induced tensile fractures (DITFs) in 46 wells throughout Brunei. Breakouts and DITFs observed in 19 wells suggest that the maximum horizontal stress is oriented margin-normal (NW-SE) in the proximal parts of the basin and margin-parallel (NE-SW) in the distal region. The margin-

parallel outer shelf stress field is interpreted as a local 'deltaic' stress field caused by the shape of the clastic wedge. The margin-normal maximum horizontal stress in the inner shelf is interpreted to reflect basement stresses associated with the active margin. However, the maximum horizontal stress in the inner shelf is perpendicular to the strike of Miocene-Pliocene normal growth faults, suggesting that maximum horizontal stress in the inner shelf has rotated from margin-parallel ('deltaic') to margin-normal ('basement-associated') over time. Hence, approximately the same stress rotation has occurred over time in the inner shelf as is currently observed spatially from the outer to inner shelf.

The spatial and temporal stress rotations in Brunei are thus interpreted to be the result of 'deltaic' and 'basement-associated' tectonic regimes that are 'prograding' basin-wards. The proximity of the active margin has resulted in progressive uplift and inversion of the hinterland that has 'forced' the delta system to prograde rapidly. The zone of active deltaic growth faulting (and margin-parallel maximum horizontal stress) has shifted basin-wards ('prograded') as the delta system has rapidly prograded across the shelf. After uplift and delta progradation, the old growth faults of the inner shelf ceased being active and have then been successively re-activated by a similarly 'prograding' margin-normal inversion front.

KEYWORDS: Brunei, *in situ* stress, deltaic tectonics.

The maximum horizontal stress (σ_{Hmax}) direction in Tertiary deltas is generally assumed to be parallel to the coastal margin due to the convex-upwards nature of the deltaic wedge (Figure 1; Yassir & Zerwer 1997). This assumption is validated by observations of borehole breakout, the formation of margin-parallel normal growth faults and structural analog modeling

(McClay 1990; Yassir & Zerwer 1997; McClay *et al.* 1998). However, the Baram Delta province is unlike classic Tertiary passive margin deltas (eg. the Mississippi and Niger Deltas) due to the proximity of the northwest Borneo active margin (Koopman & James 1996*a*). Structures within the Baram Delta province are primarily gravity-driven and deltaic in origin, but with varying degrees of compressive/transpressive interference from the active margin (Bol & van Hoorn 1980; Koopman & James 1996*b*). Furthermore, the Baram Delta province has undergone extensive exploration for hydrocarbons since 1899 (Schreurs & Ellenor, 1996). Hence, this study offers a unique opportunity to investigate the *in situ* stress in a Tertiary delta located on an active margin and in a region covered by an extensive petroleum industry database. This paper analyses the *in situ* horizontal stress orientation by interpretation of borehole breakouts and drilling-induced tensile fractures (DITFs) to determine whether the present-day stress field in Brunei is dominated by deltaic or far-field stresses associated with the active margin. The present-day stress orientations in Brunei are then compared with previous structural styles to yield a new regional interpretation of the structural evolution of the Baram Delta province.

GEOLOGICAL SETTING

The Late Neogene Baram Delta province is predominately composed of three rapidly prograding delta systems (Koopman & James 1996*a*). The Early Miocene Meligan Delta, the Early-Late Miocene (late orogenic) Champion Delta and the Late Miocene to present day Baram Delta (Figure 2). These delta systems have built outwards from the Crocker-Rajang accretionary complex and are deposited adjacent to the northwest Borneo active margin (Figure 2; Koopman & James 1996*a*). Subduction along the northwest Borneo active margin ceased in the Middle Miocene (Tan & Lamy 1980). However, collisional deformation has continued in pulses into the Quaternary (Morley *et al.* 2003). The proximity of the northwest Borneo active margin has caused extensive uplift and inversion in the proximal and eastern

parts of the basin (Figure 3; Koopman & James 1996*b*). The sub-equatorial location of the Baram Delta province resulted in the uplifted sediments being rapidly eroded, reworked and deposited further down the delta. Deposition rates within the Baram Delta province have reached 3000 m/Ma (Koopman & James 1996*b*). Rapid deposition of the fine-grained prodelta sediments has led to the development of widespread overpressures generated by disequilibrium compaction (Schreurs & Ellenor 1996; Tingay, 2003). Overpressures within the prodelta shales are commonly of sub-lithostatic magnitude and associated with undercompaction and shale diapirism (Schreurs & Ellenor 1996).

The active margin setting of the Baram Delta province has resulted in a complex interaction between gravity-driven ('thin-skinned') deltaic tectonics and transpressive/compressive ('thick-skinned') basement tectonics (Figure 4; Bol & van Hoorn 1980; Koopman & James 1996*b*). On a regional scale, the upper 15km of the Baram Delta province can be divided into three layers based on their geomechanical properties (Figure 5; Koopman & James 1996*b*):

- the brittle upper crust that acts as the 'structural basement' in Brunei (Cretaceous rocks of the Crocker-Rajang Ranges and sediments of the Meligan Delta system);
- the plastic overpressured deltaic substratum (prodelta shales), and;
- the relatively rigid deltaic overburden (deltaic sediments of the Champion and Baram Delta systems).

The style of deformation observed within the deltaic overburden is a function of the varying thickness and geomechanical properties of these three layers.

The Champion and Baram Delta systems exhibit typical deltaic structures such as growth faults, rollover anticlines and delta-toe thrust faults (Figure 4; Tan & Lamy 1990: Koopman & James 1996*b*; Morley *et al.* 2003). However, compressive and transpressive deformation in the structural basement has resulted in varying degrees of composite (basement-associated/deltaic) deformation (Figure 4). The overpressured prodelta shales act as a

decoupling zone between the structural basement and deltaic overburden. However, the thickness and amount of overpressuring (ie. rigidity) of the prodelta substratum are non-uniform (Koopman & James 1996*b*). Hence, regions with thick, highly overpressured prodelta shale sequences display classic deltaic deformation with little or no basement-associated interference (such as the outer regions of the Baram Delta system; Figure 4). In comparison, greater amounts of composite deformation are observed in uplifted and eroded areas where the prodelta shales are thinner and less overpressured, such as the proximal parts of the Champion and Baram Delta systems (Figure 4; Koopman & James 1996*b*).

DETERMINATION OF HORIZONTAL STRESS ORIENTATION

Present-day horizontal stress orientations in the Baram Delta province were determined from borehole breakouts and drilling-induced tensile fractures (DITF) interpreted from four-arm caliper and resistivity image log data. When a borehole is drilled the material removed from the subsurface is no longer supporting the surrounding rock. As a result, the stresses become concentrated in the surrounding rock (ie. the wellbore wall; Kirsch 1898). Borehole breakouts are stress-induced elongations of the wellbore and occur when the wellbore stress concentration exceeds that required to cause compressive failure of intact rock (Bell & Gough 1979). The elongation of the wellbore is the result of compressive shear failure on intersecting conjugate planes, which causes pieces of the borehole wall to spall off (Figure 6). The maximum stress around the borehole occurs perpendicular to the maximum horizontal stress in vertical boreholes (Kirsch 1898). Hence, borehole breakouts are elongated perpendicular to the maximum horizontal stress direction (Bell & Gough 1979).

Drilling-induced tensile fractures are caused by tensile failure of the borehole wall and form when the wellbore stress concentration is less than the tensile strength of the rock (Aadnoy 1990). The minimum stress around the borehole occurs in the direction of the maximum

horizontal stress in vertical boreholes (Kirsch 1898). Hence, DITFs are oriented in the σ_{Hmax} direction in vertical boreholes (Aadnoy & Bell 1998).

Breakouts are interpreted herein from Schlumberger High-resolution Dipmeter Tool (HDT) logs and resistivity image logs. The HDT is a four-arm caliper tool with two pairs of caliper arms at 90° to each other. Each arm has a pad on the end containing one or two resistivity 'buttons'. The resistivity data from the HDT log are processed to obtain information about the formation (primarily dip and strike of bedding; Schlumberger 1986). However, borehole breakouts can be interpreted from unprocessed HDT log data. The logs used to interpret breakouts from the HDT are the:

- borehole deviation (DEVI) and azimuth (HAZI);
- azimuth of pad one (P1AZ);
- bearing of pad one relative to the high side of the hole (RB), and;
- diameter of the borehole in two orthogonal directions ('caliper one' (C1) given by arms one and three and 'caliper two' (C2) from arms two and four).

The tool tends to rotate as it is pulled up the borehole due to the lay of the cable. However, the tool stops rotating where the cross-sectional shape of the borehole is elongated when one caliper pair becomes 'stuck' in the elongation direction (Figure 7; Plumb & Hickman 1985). The combined use of the six logs listed above allows the interpreter to identify zones of borehole breakout and the orientation of the elongation (Figure 7). Many non-circular wellbore cross-sectional shapes are not stress-induced, such as washout and key-seating (Plumb & Hickman 1985). Borehole breakout is distinguished from other borehole elongations on HDT logs using a strict set of criteria presented in Table 1 (Plumb & Hickman 1985).

Resistivity image logs evolved from the four-arm dipmeter logs. There are a number of resistivity buttons on each pad of the resistivity image tool, for example 16 buttons per pad on Schlumberger's Formation Micro Scanner (FMS). The multiple resistivity buttons provide an image of the borehole wall based on resistivity contrasts (Ekstrom *et al.* 1987). Resistivity image tools also measure the hole size and original logs obtained by the HDT. Several types of resistivity image tools are available. However, only Schlumberger's FMS and Formation Micro Imager (FMI) are used herein. The FMI tool is an improved version of the FMS tool that has 24 resistivity buttons on each pad and a flap attached to each pad with a further 24 buttons, thereby giving greater coverage of the wellbore wall.

The resistivity image of the wellbore wall allows for a more reliable interpretation of breakouts than could be made by using dipmeter data alone. Drilling-induced tensile fractures can also be recognised on image logs (DITFs cannot be interpreted on HDT logs). Breakouts appear on image logs as broad, parallel, often poorly resolved conductive zones separated by 180° and exhibiting caliper enlargement in the direction of the conductive zones (Figure 8a). DITFs appear on image logs as narrow, well defined, conductive fractures (Figure 8b).

Breakouts and DITFs can rotate in inclined boreholes and do not always directly yield the horizontal stress orientation (Mastin 1988; Peska & Zoback 1995). However, current state of stress in the shelf region of Brunei is believed to be a normal or strike-slip faulting stress regime (Tingay 2003; Tingay *et al*. 2003*a*). Breakouts and DITFs do not show any significant rotation in orientation and will still yield the approximate σ_{Hmax} orientation in boreholes with less than 20° deviation in a normal or strike-slip faulting stress regime (Peska & Zoback 1995). Hence, breakouts and DITFs were only used to estimate the σ_{Hmax} direction in wells with deviations of less than 20°.

The mean horizontal stress orientation from each well is given a quality ranking according to the World Stress Map Project criteria with A-quality being the highest and E-quality the lowest (Zoback 1992). Table 2 lists the quality ranking criteria for breakouts and DITFs.

RESULTS

Image logs or four-arm dipmeter logs were examined in 47 wells throughout the basin. Breakouts and/or DITFs were observed in 23 wells (Figure 9). A total of 173 breakouts and eight DITFs in 19 wells were observed in intervals with wellbore deviations of < 20°. An additional 92 breakouts and one DITF were observed in wellbores with deviations exceeding 20° and are not used herein. The observed stress-induced features indicate σ_{Hmax} is oriented approximately NW-SE in the proximal parts of the delta (the inner shelf). However, in the western outer shelf region (labeled Region A in Figure 9) breakouts and DITFs in four wells suggest an approximately NE-SW σ_{Hmax} direction.

The σ_{Hmax} orientations determined herein match other significant observations in the region. The Puffin/Parak area (near Region A) contains active normal growth faults striking NE-SW (Figure 10; Hiscott 2001). Normal growth faults typically strike in the σ_{Hmax} direction (Figure 1; Anderson 1951). Hence, the presence of active NE-SW striking growth faults in Region A is consistent with the observed σ_{Hmax} orientation from breakouts.

The margin-normal (NW-SE) σ_{Hmax} observed in the inner shelf region of Brunei agrees with σ_{Hmax} directions determined previously from borehole breakouts in northwest Borneo (Whiteley *et al.* 1991; Tija & Liew 1994; Watters *et al.* 1999). Further supporting evidence of a NW-SE σ_{Hmax} direction in the inner shelf comes from blowout fractures observed after the 1974 and 1979 blowout events in Field B. Both the 1974 and 1979 blowouts were primarily internal blowouts but resulted in several associated surface eruptions (Whiteley & Ang 1991).

An internal blowout involves overpressured fluids being transmitted along the open wellbore to shallower reservoir units rather than up the well to the surface (Figure 11). The Field B internal blowouts caused pore pressures within these shallow reservoirs to increase rapidly until the cap-rock seals to the shallow reservoirs fractured, resulting in the seabed blowouts (Figure 12; Whiteley & Ang 1991; Tingay *et al.* 2003*a*). The 1974 internal blowout was associated with a large seabed blowout and crater underneath the platform, a 600 m long string of six small craters 1000 m from the platform and a second large crater five kilometres southeast of the platform (Figure 12; Whiteley *et al.* 1991). The 1979 internal blowout was associated with two surface eruptions that expelled large volumes of overpressured fluids for ten days (Figure 12; Whiteley & Ang 1991; Koopman *et al.* 1996). Bathymetric surveys over Field B show that the 1974 and 1979 blowout craters and surface eruptions occurred in approximate straight lines oriented NW-SE (Figure 12; Whiteley *et al.* 1991). Near surface seismic amplitude time slices from high-resolution 3D seismic data in Field B reveal the presence of approximately vertical NW-SE oriented fractures underneath the crater and blowout locations (Figure 12). A similar blowout event also occurred in the onshore Seria Field in 1953. The 1953 Seria blowout was also associated with two blowout craters aligned approximately NW-SE (Whiteley *et al.* 1991).

The blowout fractures in Field B and the Seria Field can be considered analogous to large-scale hydraulic fractures, albeit initiated from an inflated reservoir rather than an inflated wellbore. Tensile fractures open against the least principal stress and, therefore, strike in the σ_{Hmax} direction in a normal or strike-slip faulting stress regime. Hence, the Field B and Seria blowout fractures are consistent with the present-day NW-SE σ_{Hmax} direction determined by borehole breakouts and DITFs in the inner shelf region of Brunei.

ORIGIN OF THE OUTER SHELF STRESS FIELD

There are several key points regarding the western outer shelf region (Region A) that are pertinent to understanding the NE-SW σ_{Hmax} orientations in the area.

(i) Region A is in the modern Baram Delta system and is an area of present-day deposition of sediments from the Baram and Belait Rivers (Schreurs & Grant 1996).

(ii) Structures within the western outer shelf region are typical deltaic features such as active margin-parallel growth faults and shale diapirs (Figure 4 & Figure 10; Koopman & James 1996*b*; Hiscott 2001).

(iii) Structures within Region A do not display any significant basement-associated deformation (as opposed to the inner shelf region; Koopman & James 1996*b*).

The stress field and associated deformation in passive margin Tertiary deltas are controlled by the geometry of the clastic wedge (Yassir & Zerwer 1997). The shape of the clastic wedge is typically convex-upward, which promotes gravity-driven extension in the delta (Figure 1; McClay 1990). Hence, Tertiary deltas on passive margins typically display growth faults and diapirs striking margin-parallel (Figure 1; Yassir & Zerwer 1997). Breakouts and DITFs also generally suggest a present-day margin-parallel σ_{Hmax} orientation in passive-margin Tertiary deltas (Figure 1; Yassir & Zerwer 1997). Hence, the current margin-parallel σ_{Hmax} direction in Region A is interpreted as a classic deltaic stress field.

ORIGIN OF THE INNER SHELF STRESS FIELD

There is an approximately 90° rotation in the present-day σ_{Hmax} direction between the margin-parallel deltaic stress field in Region A and the margin-perpendicular (NW-SE) σ_{Hmax} direction observed in the inner shelf region of Brunei. Hence, an additional (non-deltaic) source of stress is influencing the stress field in the deltaic sediments of the inner shelf. There

are several key points regarding the inner shelf region that are pertinent to understanding the NW-SE stress orientations in the area.

(i) Inner shelf sediments are older sequences of the Baram and Champion Delta systems (predominately Middle Miocene to Pliocene).

(ii) Structures in the inner shelf are primarily deltaic such as margin-parallel growth faults, roll-over anticlines and shale diapirs (Koopman & James 1996*b*).

(iii) Basement-associated deformation of the deltaic structures is common in the inner shelf (Koopman & James 1996*b*).

(iv) The hinterland of the Baram Delta province has been variably uplifted with uplift increasing proximally (Tingay *et al.* 2003*b*).

(v) There has been Late Miocene and Pliocene inversion of normal faults in most inner shelf fields (Morley *et al.* 2003).

(vi) The pro-delta shales are older and thinner in the inner shelf and allow greater 'attachment' of the deltaic sequences to the structural basement (Koopman & James 1996*b*).

(vii) No active faulting or seismicity has been observed in the inner shelf (Leong 1999).

The basement-associated deformation, uplift of the hinterland and inversion in several fields suggests that the present-day σ_{Hmax} direction in the inner shelf deltaic sediments may be associated with the regional or far-field stresses in the structural basement. There is no data known to the author regarding the *in situ* stress field in the structural basement underlying the Baram Delta province. However, several pieces of evidence support the hypothesis of an approximate NW-SE present-day σ_{Hmax} direction in the structural basement.

The first-order (plate-scale) σ_{Hmax} direction is typically in the direction of plate motion (Zoback 1992). The plate motion in Brunei is poorly constrained from static GPS surveys, but it is believed to be approximately east-southeast (120°N; Michel *et al.* 2000).

Borehole breakouts in the Ocean Drilling Program (ODP) well 1143A suggest an approximate WNW-ESE present-day σ_{Hmax} direction on the northwest side of the northwest Borneo Trough (from an FMS log interpreted by the author). ODP well 1143A is located at 9° 21.7'N, 113° 17.1'E (in the South China Sea approximately 600 km of Brunei) in 2782 m water depth. The well was drilled to 400 m below seabed into Miocene-Recent hemipelagic sediments directly overlying structural basement (Wang *et al.* 1999). Two earthquake focal mechanism solutions from the central South China Sea also suggest a NW-SE present-day far-field σ_{Hmax} direction (Reinecker *et al.* 2003).

Hutchinson (1989) suggests that the current σ_{Hmax} direction in the basement is likely to be NW-SE from recent structural trends observed throughout northwest Borneo. Furthermore, the major Pliocene inversion events affecting the Champion, Miri, Seria, Ampa and Iron Duke-Bugan anticlines were caused by 'pulses' of NW-SE basement-associated compression (Watters *et al.* 1999; Morley *et al.* 2003).

Given the above evidence that the σ_{Hmax} orientation in the basement underlying the Baram Delta province is likely to be approximately NW-SE, the NW-SE σ_{Hmax} direction in the inner shelf is interpreted to be the result of far-field and/or basement stresses transmitted through the prodelta shales into the deltaic overburden.

MAXIMUM HORIZONTAL STRESS ROTATION IN BRUNEI

The rotation of the present-day σ_{Hmax} direction in the Baram Delta province is interpreted as the result of two competing orthogonal stress fields:

- a 'local' margin-parallel (NE-SW) deltaic σ_{Hmax} orientation caused by the shape of the clastic wedge, and;

- a NW-SE (margin-normal) σ_{Hmax} orientation most likely related to basement or first-order stresses transmitted through the pro-delta shales.

The orientation of σ_{Hmax} in a field or region is controlled by whichever of these two stress fields is dominant.

It is of particular interest that the present-day stress orientation in the inner shelf is inconsistent with structural styles observed on seismic data and in outcrop in the area. This is very much in contrast with the classic passive margin delta pattern where present-day σ_{Hmax} orientations and structural development are consistent (Figure 1; Yassir & Zerwer 1997). The present-day σ_{Hmax} orientation in the inner shelf is margin-normal. However, the structures observed in the inner shelf are primarily margin-parallel deltaic features such as growth faults, rollover anticlines and shale diapirs (albeit with basement-associated interference and inversion; Figure 9). Present-day σ_{Hmax} acts normal to the strike of extensional growth faults in the inner shelf and is inconsistent with the development of these structures (Figure 9). The prevalence of deltaic structures in the inner shelf suggests that a deltaic margin-parallel σ_{Hmax} direction was previously dominant in the inner shelf. Hence, there has been an approximately 90° rotation in the σ_{Hmax} direction over time from that associated with deltaic tectonics to the present-day basement-associated stress field.

Shale dykes in the Jerudong Anticline provide further evidence of the temporal σ_{Hmax} rotation in the inner shelf. Some shale dykes have failed in tension and are analogous to natural hydraulic fractures (Figure 13**a**). Other shale dykes occur in fault planes that were presumably active at the time of injection (Figure 13**b**; Sibson 1996; Morley *et al.* 1998). The Middle Miocene shale dykes in the Jerudong Anticline predominantly strike NE-SW after rotation to their pre-folding orientation (Morley *et al.* 1998). Hence, the shale dykes suggest a margin-parallel σ_{Hmax} direction associated with a deltaic stress field during the Middle Miocene in the Jerudong Anticline. However, shale dykes in the Jerudong Anticline that were emplaced

during the Pliocene strike NW-SE (Figure **13a**). Thus, the Pliocene shale dykes suggest a NW-SE, margin-normal σ_{Hmax} direction and supports the rotation of σ_{Hmax} over time in the inner shelf.

The present-day stress field of the Baram Delta province is thus interpreted to reveal both spatial and temporal rotations in σ_{Hmax} direction (when compared to earlier deformations):

- the rotation of present-day σ_{Hmax} from margin-normal in the inner shelf to the margin-parallel in the outer shelf (spatial), and;
- the rotation of σ_{Hmax} in the inner shelf from Miocene, deltaic, and margin-parallel to its present-day, basement-associated, and margin-normal orientation (temporal).

'PROGRADING DELTAIC TECTONICS': A REGIONAL INTERPRETATION OF THE STRUCTURAL EVOLUTION OF THE BARAM DELTA PROVINCE

The temporal and spatial rotations of σ_{Hmax} orientation in the Baram Delta province are interpreted herein to be the result of 'prograding deltaic tectonics' in the region. The inner shelf has been subject to the following general sequence of events (Figure 14; Morley *et al.* 2003).

1. Deposition of deltaic sediments with associated deltaic tectonics (σ_{Hmax} margin-parallel).
2. Uplift of the hinterland causing deltaic deposition to shift distally and hence, deltaic deformation to cease.
3. Inversion of growth faults, regional uplift and erosion (ie. basement-associated tectonics; predominately σ_{Hmax} margin-normal).

Deltaic growth faulting (and the associated deltaic stress field) is syn-depositional and localised in the region of deltaic deposition (Tearpock & Bischke 2003). The uplift of the

hinterland has ‘forced’ the rapid progradation of the Baram and Champion Delta systems. Therefore, the deltaic deformation observed in the Baram Delta province has generally shifted distally over time (Figure 14). Deltaic deformation has moved gradually from Middle Miocene faulting and diapirism near Jerudong, Seria and the eastern inner shelf region to the present-day growth faulting in the western outer shelf region (Figure 14; Koopman & James 1996*b*; Morley *et al.* 2003). Hence, the deltaic tectonics and the associated deltaic stress field have ‘prograded’ basin-ward as the delta has built outwards across the shelf. (Figure 14).

Many fields and structures in the inner shelf have undergone uplift and inversion after the initial deltaic deposition and deformation (Koopman *et al.* 1996). These inversion events have occurred in progressively basin-ward regions over time (Figure 14; Morley *et al.* 2003). Inversion first occurred in the Jerudong Anticline and along the Muara fault zone in the Middle Miocene (Morley *et al.* 2003). The earliest inversion events lead to the development of N-S trending structures and are believed to be the result of approximately E-W compression (Morley *et al.*, 2003). Inversion continued in the Jerudong Anticline and began in the Belait region and Field B in the late Middle Miocene (Morley *et al.* 2003). The mixed N-S and NE-SW trend of inversion structures formed during the late Middle Miocene and Late Miocene suggests a rotation in σ_{Hmax} from E-W to the more NW-SE orientation observed in the present-day. Late Miocene inversion was primarily in the Belait region with minor inversion events in the Scout Rock, Magpie and Iron Duke Fields (Koopman & James 1996*b*; Morley *et al.* 2003). The Miri, Seria, Champion, Ampa, Magpie and Labuan Anticlines and the Punyit/Kenari and Iron Duke/Bugan regions all underwent NW-SE oriented Pliocene inversion (Koopman & James 1996*b*; Morley *et al.* 2003). Hence, the basin-ward ‘prograding’ gravity-driven deltaic deformation has been ‘followed’ by a similarly ‘prograding’ zone of inversion events (Figure 14).

CONCLUSIONS

This paper is the first detailed study known to the authors of present-day stress in a Tertiary delta on an active margin and thus, provides a unique insight into the tectonic development of rapidly prograding delta systems. The Baram Delta province exhibits a margin-normal basement-associated stress field in addition to a margin-parallel deltaic stress field. Hence, the stress field in the Baram Delta province is inconsistent with the purely margin-parallel deltaic stress fields observed in Tertiary deltas on passive margins. Furthermore, comparison of structural styles with the present-day stress field reveals that both the margin-parallel deltaic and margin-normal basement-associated stress fields have 'prograded' basin-wards over time as the delta has built outwards. Hence, the rotation of present-day σ_{Hmax} orientation from the inner to the outer shelf yields a 'snapshot' of the interpreted 'prograding deltaic tectonics' in the Baram Delta province – the dynamic structural evolution of a rapidly prograding Tertiary delta system deposited on an active margin captured in a single geological 'instant'.

REFERENCES

Aadnoy, B. S. 1990. In-situ stress direction from borehole fractures. *Journal of Petroleum Science and Engineering*, **4**, 143-153.

Aadnoy, B. S. & Bell, J. S. 1998. Classification of drill-induce fractures and their relationship to in-situ stress directions. *The Log Analyst*, **39**, 27-42.

Anderson, E. M. 1951. *The dynamics of faulting and dyke formation*. London, Oliver and Boyd.

Bell, J. S. & Gough, D. I. 1979. Northeast-southwest compressive stress in Alberta: Evidence from oil wells. *Earth and Planetary Science Letters*, **45**, 475-482.

Bol, A. J. & van Hoorn, B. 1980. Structural styles in Western Sabah offshore. *Geological Society of Malaysia Bulletin*, **12**, 1-16.

Ekstrom, M. P., Dahan, C. A., Chen, M. Y., Lloyd, P. M. & Rossi, D. J. 1987. Formation imaging with microelectrical scanning arrays. *The Log Analyst*, **28**, 294-306.

Hiscott, R. N. 2001. Depositional sequences controlled by high rates of sediment supply, sea-level variations, and growth faulting: the Quaternary Baram Delta of northwestern Borneo. *Marine Geology*, **175**, 67-102.

Hutchinson, C. S. 1989. *Geological evolution of Southeast Asia*. Oxford, Clarendon Press.

Kirsch, V. 1898. Die Theorie der Elastizität und die Beddürfnisse der Festigkeitslehre. *Zeitschrift des Vereines Deutscher Ingenieure*, **29**, 797-807.

Koopman, A., Schreurs, J. & Ellenor D. W. 1996. Chapter 5: The Oil and Gas Resources of Brunei. *In*: Sandal, S. T. (ed) *The Geology and Hydrocarbon Resources of Negara Brunei Darussalam*. Bandar Seri Begawan, Syabas, 155-192.

Koopman, A. & James, D. M. D. 1996*a*. Chapter 2: Regional Geological Setting. *In*: Sandal, S. T. (ed) *The Geology and Hydrocarbon Resources of Negara Brunei Darussalam*. Bandar Seri Begawan, Syabas, 49-63.

Koopman, A. & James, D. M. D. 1996*b*. Chapter 3: Structure. *In*: Sandal, S. T. (ed) *The Geology and Hydrocarbon Resources of Negara Brunei Darussalam*. Bandar Seri Begawan, Syabas, 64-80.

Leong, W. F. 1999. Brunei Darussalam - Country Report. *WWSI Workshop on Seismic Risk Management II*, 25-33.

Mastin, L. 1988. Effect of borehole deviation on breakout orientations. *Journal of Geophysical Research*, **93**, 9187-9195.

McClay, K. R., 1990, Extensional fault systems in sedimentary basins: a review of analogue model studies: Marine and Petroleum Geology, v. 7, p. 206-233.

McClay, K. R., Dooley, T. & Lewis, G. 1998. Analogue modeling of progradational delta systems. *Geology*, **29**, 771-774.

Michel, G. W., Becker, M., Angermann, D., Reigber, C. & Reinhart, E. 2000. Crustal motion in E- and SE-Asia from GPS measurements. *Earth Planets Space*, **52**, 713-720.

Morley, C. K., Crevello, P. & Ahmad, Z. H. 1998. Shale tectonics and deformation associated

with active diapirism: the Jerudong Anticline, Brunei Darussalam. *Journal of the Geological Society, London*, **155**, 475-490.

Morley, C. K., Back, S., Crevello, P., van Rensbergen, P. & Lambiase, J. J. 2003. Characteristics of repeated, detached, Miocene-Pliocene tectonic inversion events, in a large delta province on an active margin, Brunei Darussalam, Borneo. *Journal of Structural Geology*. **25**, 1147-1169.

Peska, P. & Zoback, M. D. 1995. Compressive and tensile failure of inclined well bores and determination of *in situ* and rock strength. *Journal of Geophysical Research*, **100**, 12791-12811.

Plumb, R. A. & Hickman, S. H. 1985. Stress-induced borehole elongation: A comparison between the Four-Arm Dipmeter and the Borehole Televiewer in the Auburn Geothermal Well. *Journal of Geophysical Research*, **90**, 5513-5521.

Reinecker, J., Heidbach, O. & Mueller, B. 2003. *The 2003 release of the World Stress Map* (available online at www.world-stress-map.org)

Schlumberger. 1986. *Dipmeter Interpretation*. New York, Schlumberger Limited.

Schreurs, J. & Grant, C. K. 1996. Chapter 1: Geographical Overview. *In*: Sandal, S. T. (ed) *The Geology and Hydrocarbon Resources of Negara Brunei Darussalam*. Bandar Seri Begawan, Syabas, 22-48.

Schreurs, J. & Ellenor, D. W. 1996. Chapter 5: The Oil and Gas Resources of Brunei Darussalam - Hydrocarbon Habitat. *In*: Sandal, S. T. (ed) *The Geology and Hydrocarbon Resources of Negara Brunei Darussalam*. Bandar Seri Begawan, Syabas, 130-154.

Sibson, R. H. 1996. Structural permeability of fluid-driven fault-fracture meshes. *Journal of Structural Geology*, **18**, 1031-1042.

Tan, D. N. K. & Lamy, J. M. 1990. Tectonic evolution of the NW Sabah continental margin since the Late Eocene. *Geological Society of Malaysia Bulletin*, **27**, 241-260.

Tearpock, D. J. & Bischke, R. E. 2003. *Applied Subsurface Geological Mapping with Structural Methods*. New Jersey, Pearson Education, Ltd.

Tija, H. D. & Liew, K. K. 1994. Tectonic implications of well-bore breakouts in Malaysian basins. *Geological Society of Malaysia Bulletin*, **36**, 175-186.

Tingay, M. R. P. 2003. *In situ stress and overpressures of Brunei Darussalam*. PhD thesis, University of Adelaide.

Tingay, M. R. P., Hillis, R. R., Morley, C. K., Swarbrick, R. E. & Okpere E. C. 2003*a*. Pore pressure-stress coupling in Brunei Darussalam - implications for shale injection. *In:* van Rensbergen, P., Hillis, R. R., Maltman, A. J. & Morley C. K. (eds) *Subsurface Sediment Mobilization*. Geological Society, London, Special Publications, **216**, 369-379.

Tingay, M. R. P., Hillis, R. R., Morley, C. K., Swarbrick, R. E. & Okpere E. C. 2003*b*. Variation in vertical stress in the Baram Basin, Brunei: tectonic and geomechanical implications. *Marine and Petroleum Geology*, **20**, 1201-1212.

Wang, P., Prell, W. L. & Blum, P. 2000. *Proceedings of the Ocean Drilling Program, Initial Reports, Leg 184*.

Watters, D. G., Maskall, R. C., Warrilow, I. M. & Liew, V. 1999. A sleeping giant awakened: further development of the Seria Field, Brunei Darussalam, after almost 70 years of production. *Petroleum Geoscience*, **5**, 147-159.

Whiteley, S. L. & Ang, S. L. 1991. Champion-141 Internal Blowout Procedures Guide. Brunei Shell Petroleum Report.

Whiteley, S. L., Yuk, B. P. & Schaafsma, C. E. 1991. Blowout cratering and principal stress orientations in the Champion Field. Brunei Shell Petroleum Report.

Yassir, N. A. & Zerwer A. 1997. Stress regimes in the Gulf Coast, offshore Louisiana: data from well-bore breakout analysis. *American Association of Petroleum Geologists Bulletin*, **81**, 293-307.

Zoback, M. L. 1992. First- and second-order patterns of stress in the lithosphere: The world stress map project. *Journal of Geophysical Research*, **97**, 11703-11728.

The authors would like to thank Brunei Shell Petroleum for the data used in this research and the Australian Research Council for funding this project.

TABLES

1. Tool rotation must cease in the zone of elongation (maximum of 15° rotation within breakout).
2. There must be clear tool rotation into and out of the elongation zone (at least 30°).
3. The difference between caliper extensions must be > 6 mm.
4. The smaller of the caliper readings must be very close to bit size (±5% tolerance).
5. The length of the elongation zone must be > 1 m
6. The elongation orientation should not coincide with the high side of the borehole in wells deviated by more than 5° (±5° tolerance).

Table 1. *Criteria for recognizing breakouts on 4-arm caliper (HDT) logs and as applied herein (Plumb & Hickman 1985)*

A-Quality	B-Quality	C-Quality	D-Quality	E-Quality
Ten or more distinct breakout zones in a single well with s.d. ≤ 12° and/or combined length > 300 m	At least six distinct breakout zones in a single well with s.d. ≤ 20° and/or combined length > 100 m	At least four distinct breakouts with s.d. ≤ 25° and/or combined length > 30 m	Less than four breakouts or < 30 m combined length or breakouts in well have s.d. > 25°	Wells in which no reliable breakouts detected or extreme scatter of breakout orientations (s.d. > 40°)

Table 2. *World Stress Map (WSM) Project quality ranking criteria for breakouts (Zoback 1992). There are no WSM criteria for quality ranking of DITFs. Herein, the above criteria were also used for DITFs. s.d. = standard deviation.*

FIGURE CAPTIONS

Figure 1. Relationship between deltaic structures (growth faults and diapirs), borehole breakouts, DITFs and the present-day stress field in the Mississippi Delta (a typical passive margin Tertiary delta). The convex-upwards geometry of the clastic wedge promotes gravity-driven extension in the delta. Hence, σ_{Hmax} is usually oriented margin-parallel in Tertiary deltas (adapted from Yassir & Zerwer 1997).

Figure 2. Map of northern Borneo showing location of the three major delta systems of the Baram Delta province (adapted from Koopman & James 1996*a*), Crocker-Rajang accretionary complex and the northwest Borneo active margin (expressed in the present-day by the outer zone of thrusting and the northwest Borneo trough).

Figure 3. Schematic cross-section of Brunei illustrating the successive prograding deltaic systems and relationship between pro-delta shales and deltaic sediments (adapted from Koopman & James 1996*a*). Note that proximal parts of the delta province have been uplifted, eroded and re-worked sediments deposited further down the delta system.

Figure 4. Major structures in Brunei including locations of major shale diapirs (shaded dark grey; adapted from Koopman & James 1996*b* and Morley *et al.* 2003).

Figure 5. Major geomechanical layers of subsurface Brunei (adapted from Koopman & James 1996*b*).

Figure 6. Results of a hollow cylinder lab test simulating borehole breakout (performed by the CSIRO Division of Geomechanics). Note the conjugate shear failure planes resulting in ovalisation of the cross-sectional shape of the wellbore.

Figure 7. HDT log plot from offshore Brunei displaying borehole breakout. Caliper one (C1) locks into breakout zone from 2895-2860 m (P1AZ≈200°N) then the tool rotates 90° and caliper two (C2) locks into another breakout from 2845-2835 m (P1AZ≈290°N). Both breakout zones are oriented approximately 020°N and suggest a σ_{Hmax} direction of 110°N. The wellbore is deviated 4° towards 140°N.

Figure 8. FMI resistivity images from offshore Brunei showing (**a**) borehole breakout and (**b**) drilling-induced tensile fractures.

Figure 9. Present-day maximum horizontal stress orientations in Brunei. Length of each indicator is representative of stress indicator quality (as per Table 2). Maximum horizontal stress is oriented approximately margin-parallel in the outer shelf (Region A) and approximately margin-normal in the inner shelf.

Figure 10. Shallow seismic section across a growth fault near the Puffin/Parak Field (from Hiscott 2001). Note the 15 m high fault scarp indicating the fault is active

Figure 11. Schematic diagram of the Field B internal blowouts and associated surface eruptions (adapted from Whiteley *et al.* 1991).

Figure 12. Near surface seismic amplitude time-slice across Field B. 1974 and 1979 blowout craters and surface eruption locations are outlined in white and overlie two NW-SE trending sub-vertical fractures (highlighted in black).

Figure 13. Shale dykes in the Jerudong Anticline. (**a**) Pliocene shale dyke injected along a tensile fracture. (**b**) shale dyke injected along a fault plane. Middle to Late Miocene shale dykes generally strike NE-SW (after rotation to their pre-folding orientation). Hence, the shale dykes suggest a NE-SW σ_{Hmax} direction in the Middle to Late Miocene (Morley et al. 1998). Pliocene shale dykes strike NW-SE suggesting a margin-normal σ_{Hmax} and indicating a temporal rotation from a 'deltaic' to 'basement-associated' stress field.

Figure 14. Evolution of structures in the Baram Delta province from Middle Miocene to present (structural history adapted from Koopman & James 1996*b* and Morley *et al.* 2003). Zones of hinterland uplift, deltaic tectonics and inversion have 'prograded' over time. Red shaded regions are areas of major shale diapirism.

FIGURES

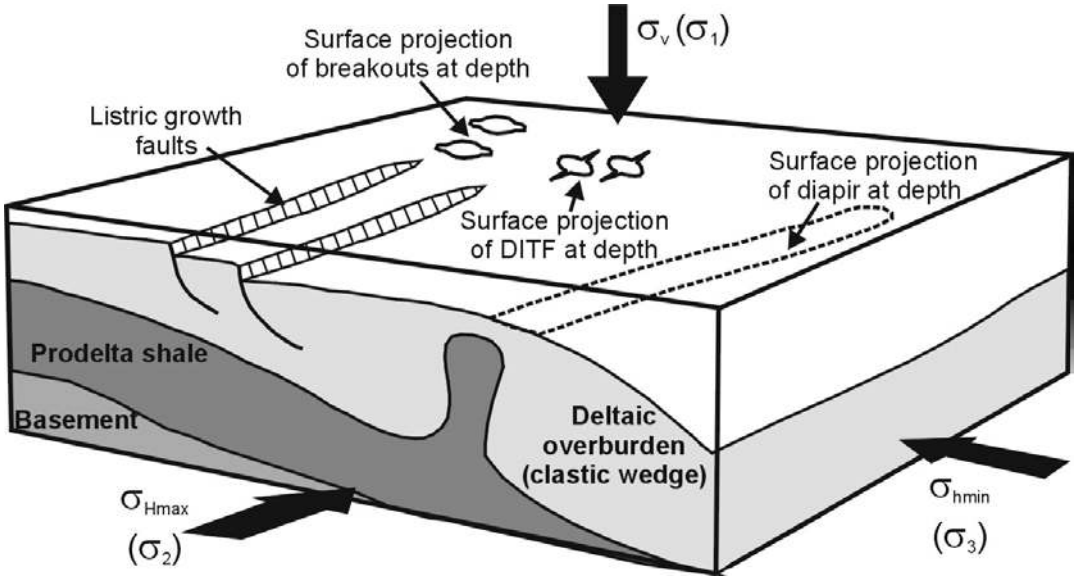

Figure 1

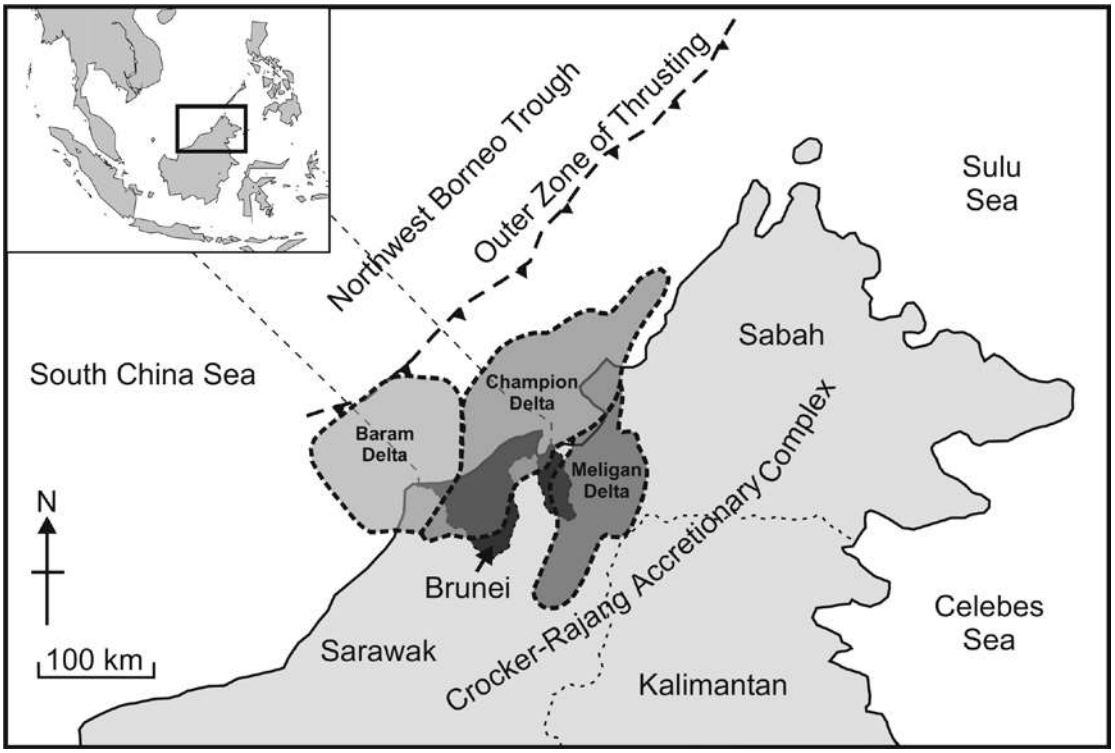

Figure 2

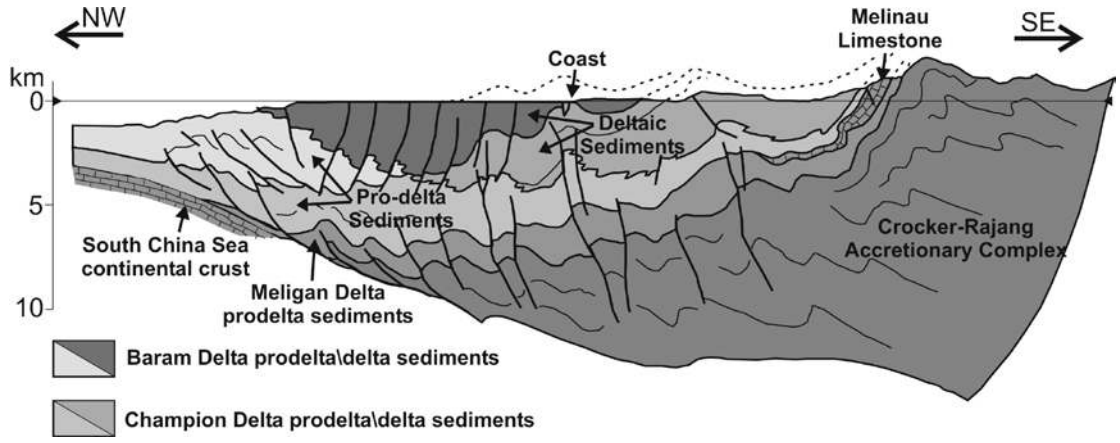

Figure 3

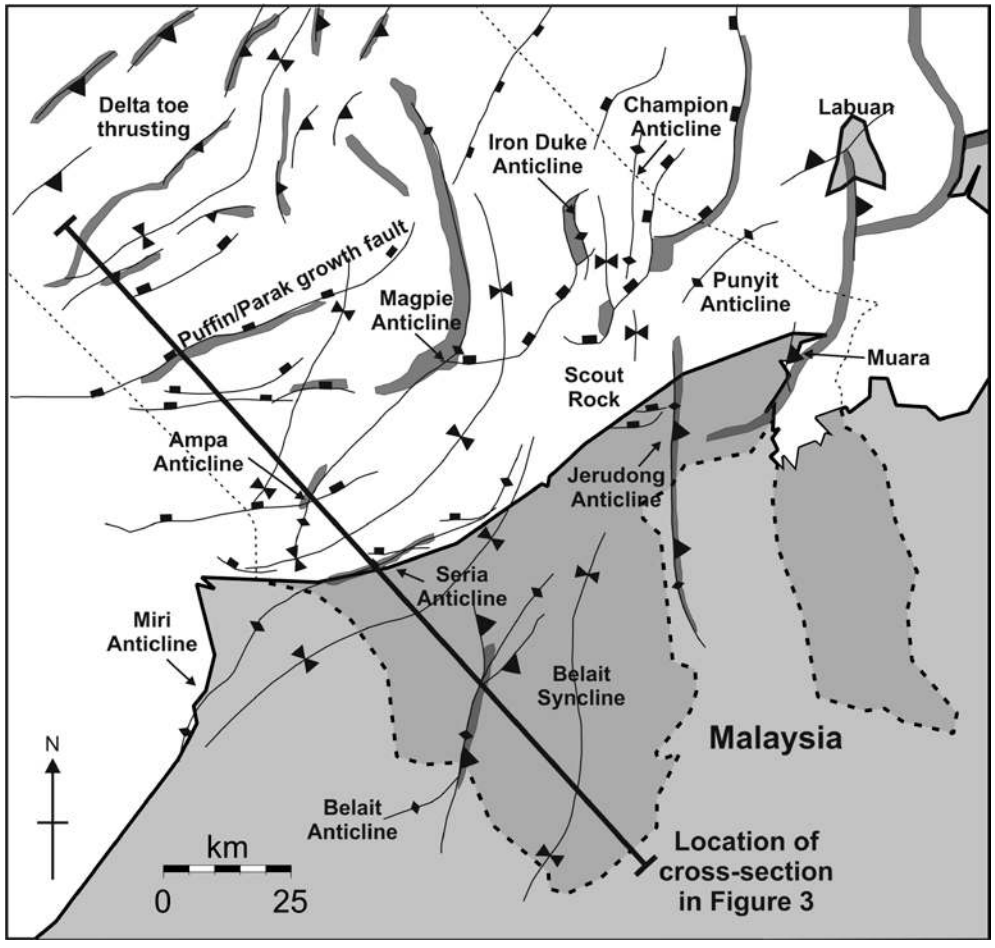

Figure 4

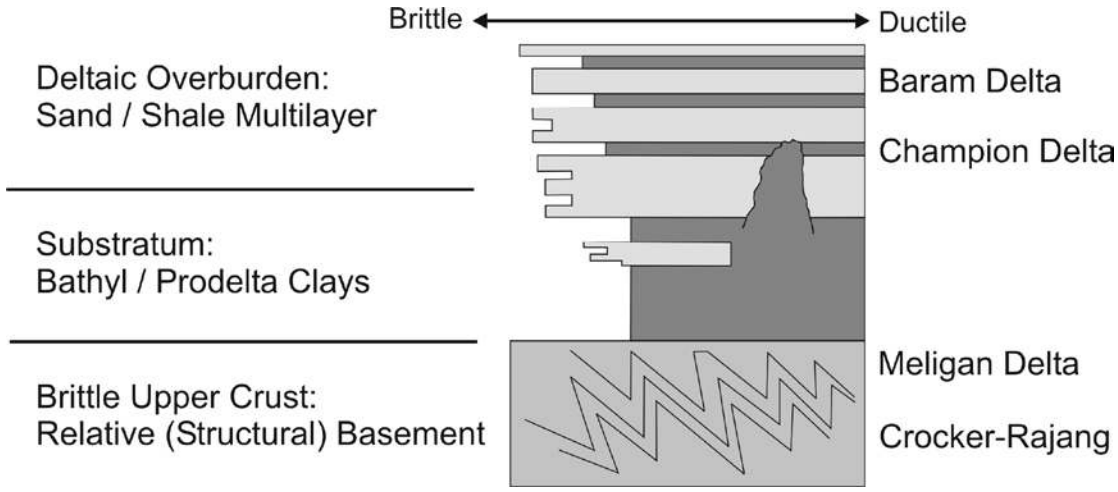

Figure 5

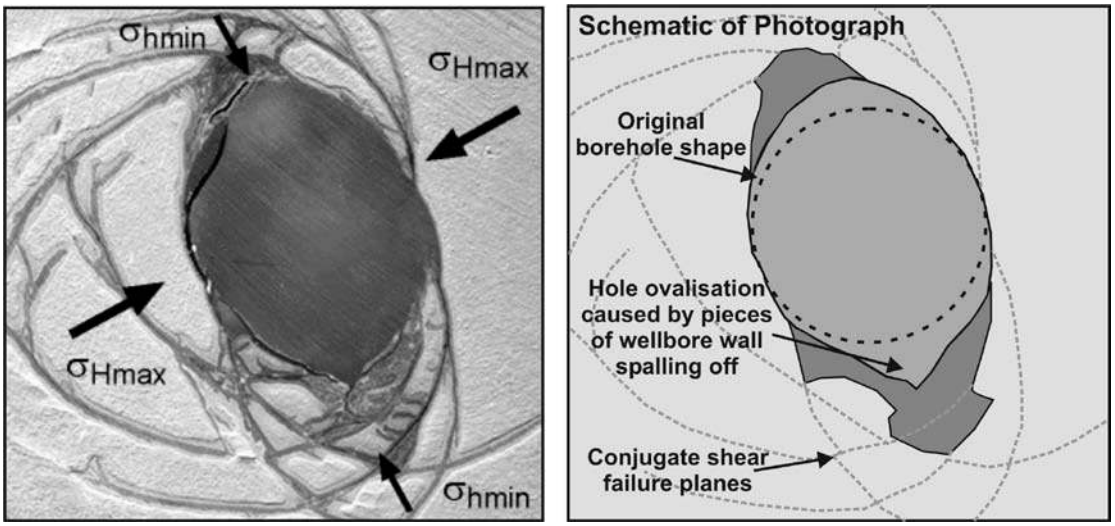

Figure 6

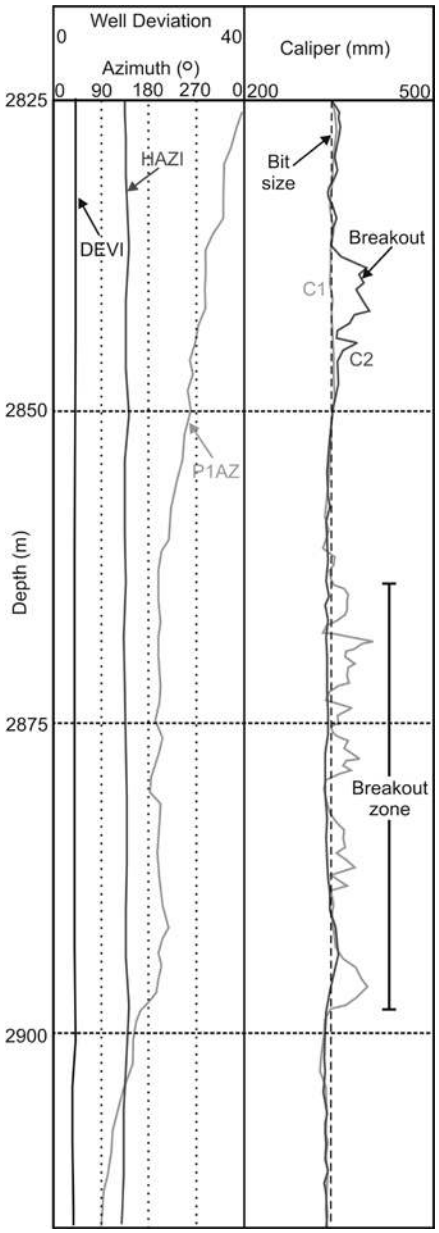
Well Deviation
0
40
Azimuth (°)
0 90 180 270 0
Caliper (mm)
200 500
2825
2850
2875
2900
Depth (m)
HAZI
DEVI
P1AZ
Bit size
Breakout
C1
C2
Breakout zone

Figure 7

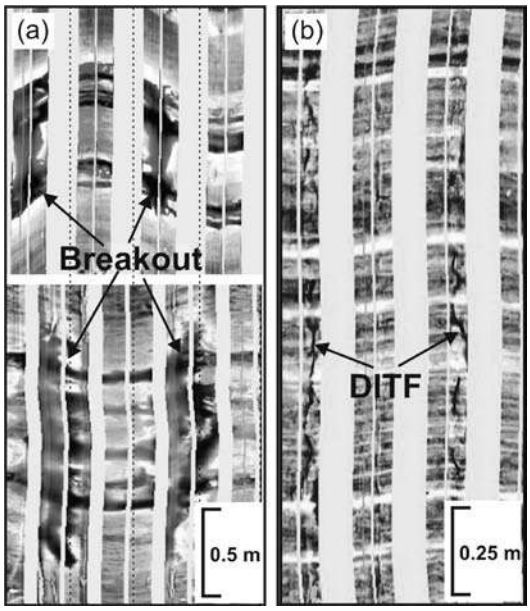

Figure 8

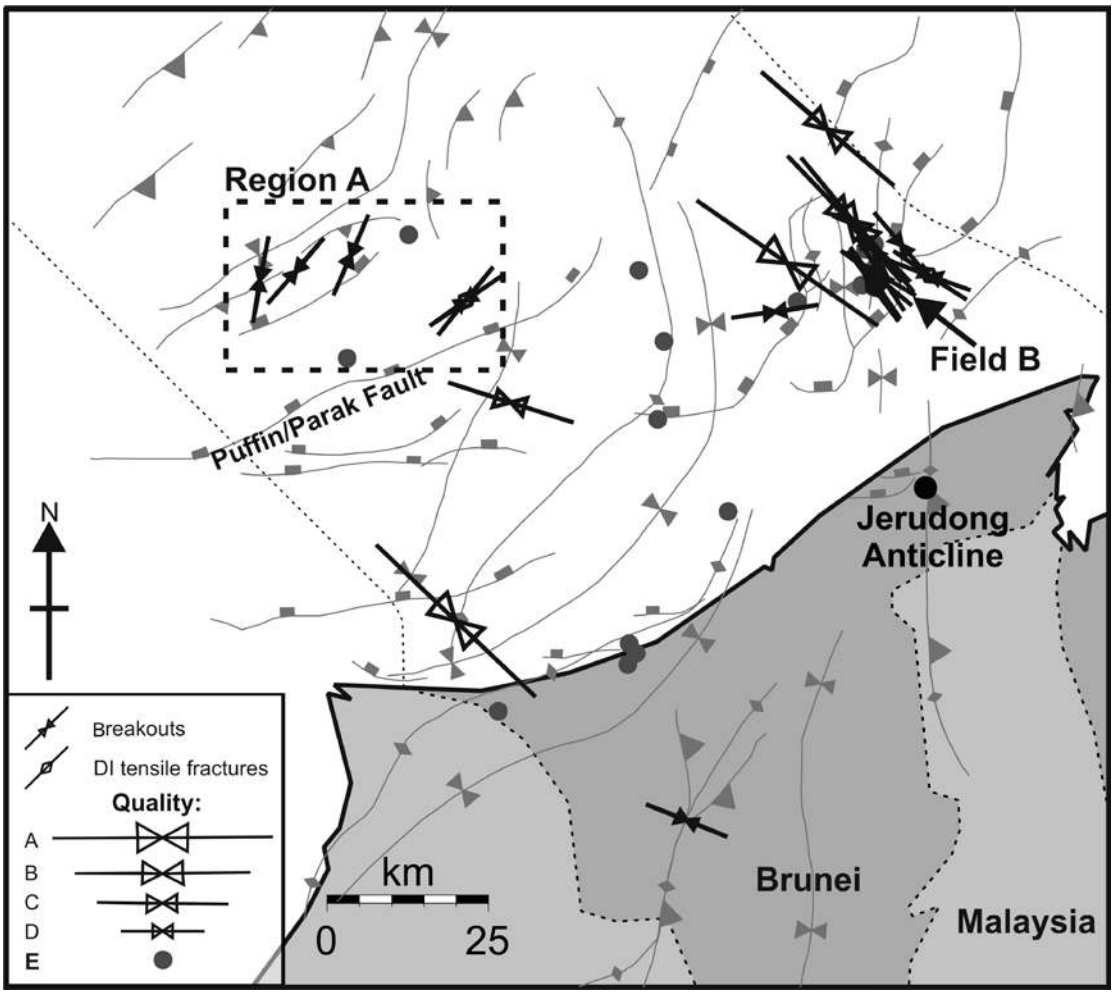

Figure 9

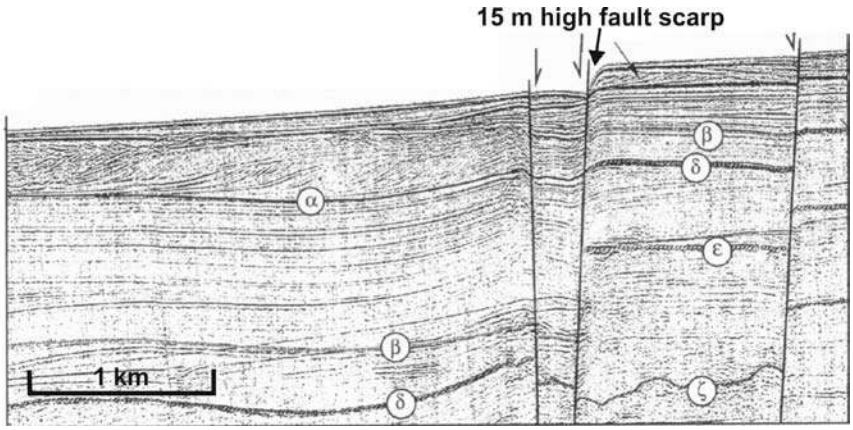

Figure 10

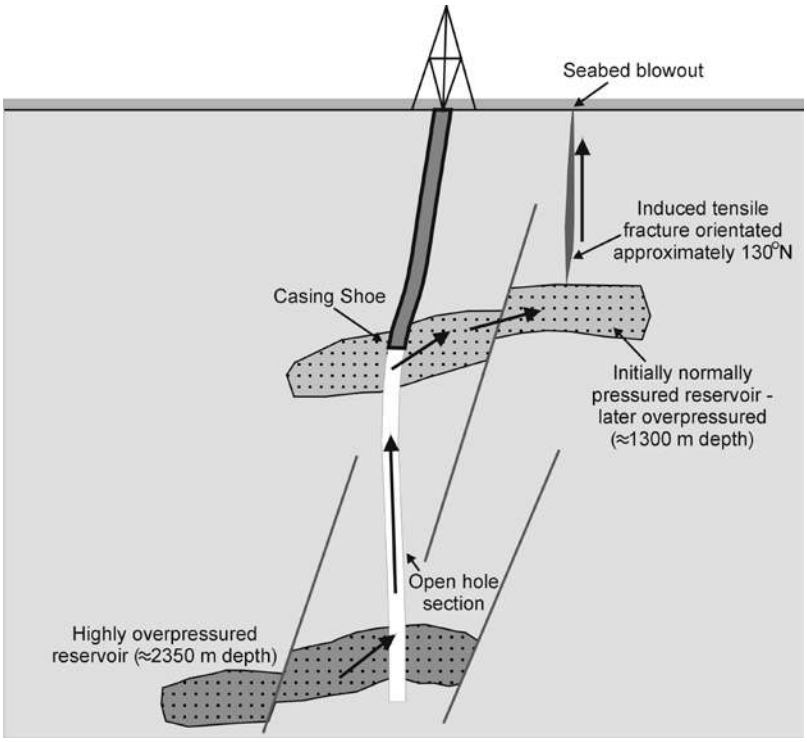

Figure 11

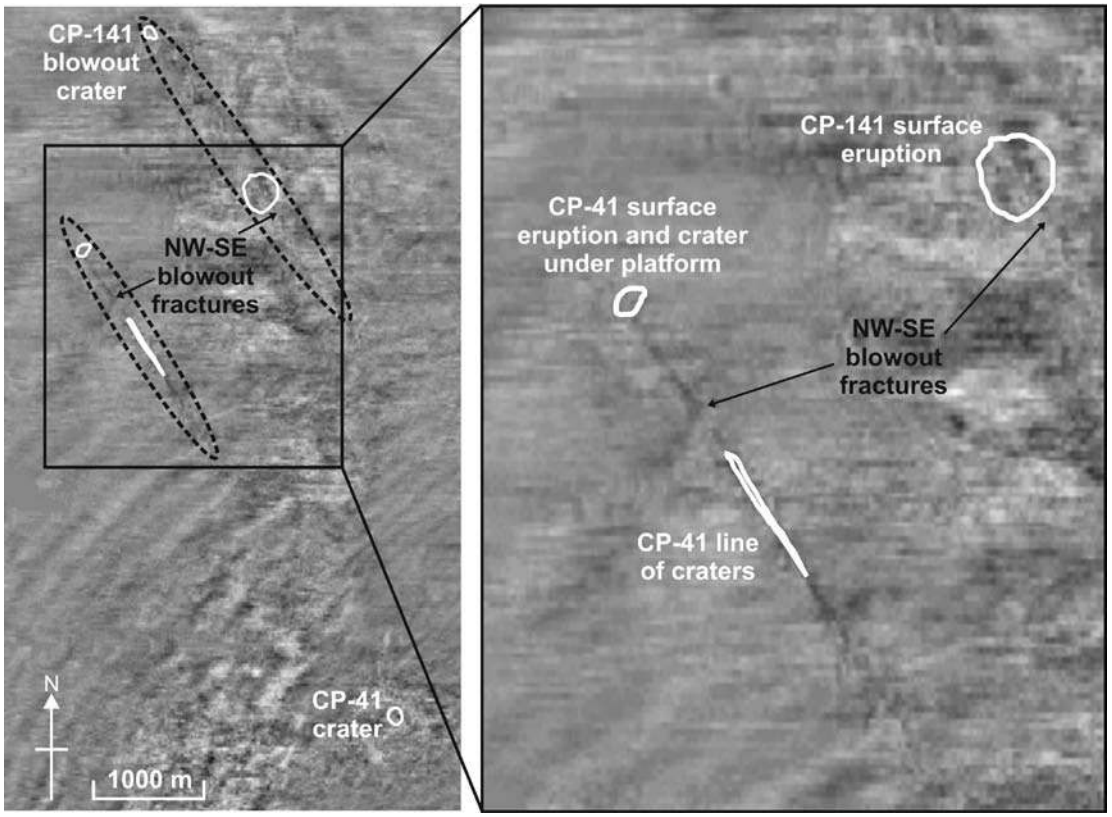

Figure 12

Figure 13

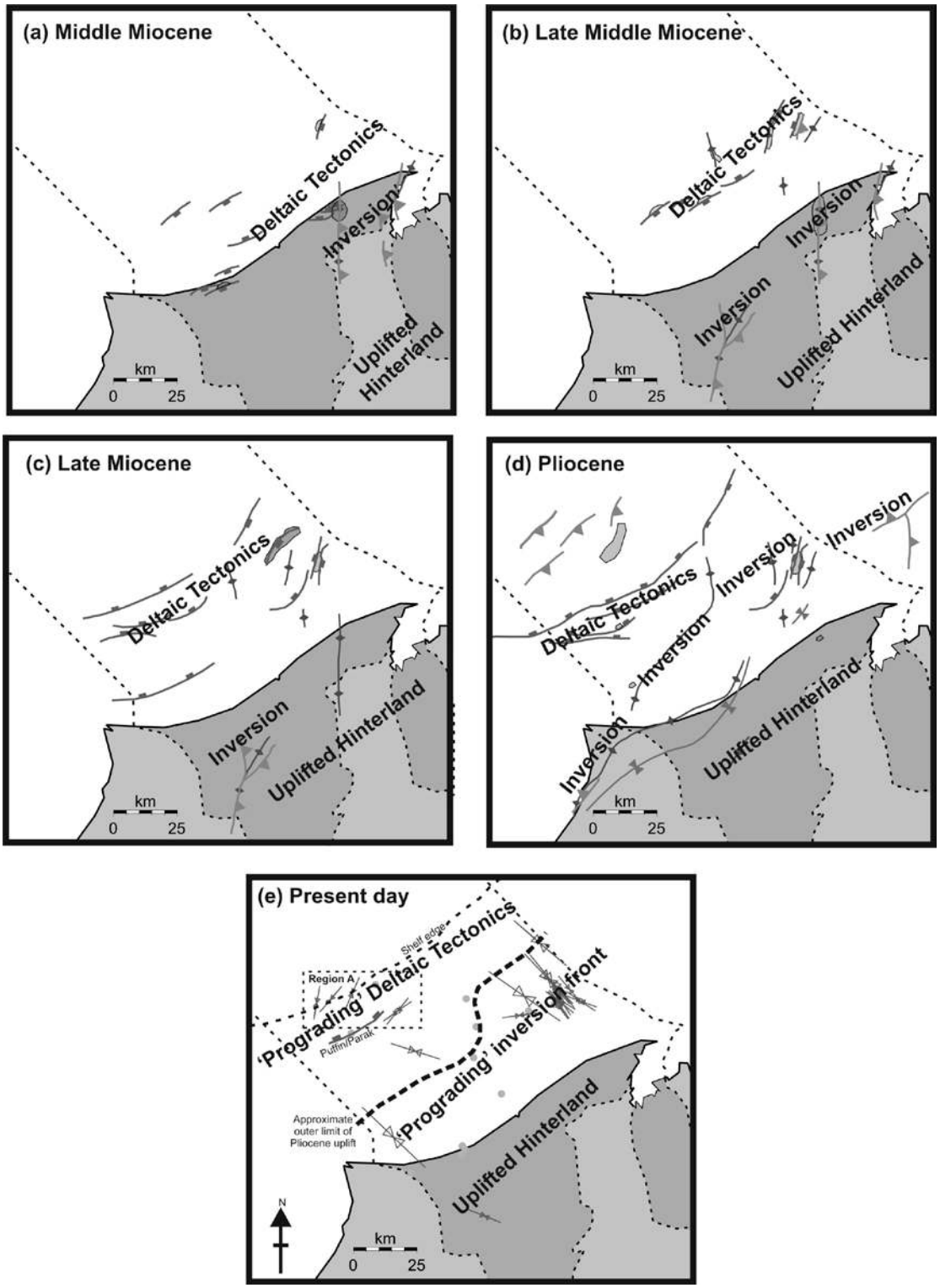
(a) Middle Miocene
Deltaic Tectonics
Inversion
Uplifted Hinterland
km
0 25
(b) Late Middle Miocene
Deltaic Tectonics
Inversion
Inversion
Uplifted Hinterland
km
0 25
(c) Late Miocene
Deltaic Tectonics
Inversion
Uplifted Hinterland
km
0 25
(d) Pliocene
Deltaic Tectonics
Inversion
Inversion
Inversion
Inversion
Uplifted Hinterland
km
0 25
(e) Present day
Shelf edge
Region A
'Prograding' Deltaic Tectonics
Puffin/Parak
'Prograding' inversion front
Approximate outer limit of Pliocene uplift
Uplifted Hinterland
N
km
0 25

Figure 14